JOURNAL OF
NATURAL SCIENCES AND MATHEMATICS RESEARCH

Available online at http://journal.walisongo.ac.id/index.php/jnsmr

Identification of the Subsurface Structure of Geothermal Working Area of the Hamiding Mountain, North Maluku through Land Surface Temperature (LST) Data and Forward Modeling with the Gravity Method

Muhammad Nafian[1*], Belista Gunawan[1], Nanda Ridki Permana[2], and Rofiqul Umam[3]
[1]Program Study of Physics, Faculty of Science and Technology, Universitas Islam Negeri Syarif Hidayatullah Jakarta, Jalan. Ir. H. Djuanda No.95, Cempaka Putih, Ciputat, Kota Tangerang Selatan, Banten 15412, Indonesia
[2]PT. Minelog Service Indonesia, BSD, Bumi Serpong Damai, Kawasan Industri & Gudang Taman Tekno Blok G1 No. 10, Jl. Sektor 11, Setu, Kec. Setu, Kota Tangerang Selatan, Banten 15220, Indonesia
[3]Department of Applied Chemistry for Environment, Kwansei Gakuin University, 669-1330 Gakuen Uegahara 1 Chome Sanda Shi, Hyogo Prefecture, Japan

Corresponding author:
Muhammad.nafian@uinjkt.ac.id
Received : 10 Jan 2022
Revised : 10 May 2022
Accepted : 25 June 2022

Abstracts

The Mount Hamiding area has one of the largest geothermal potentials in Indonesia to be exploited. Therefore, this research was conducted with the aim of knowing the subsurface structure in the area using the gravity method. To correlate gravity data in order to obtain parameters to measure the increase in surface temperature using supporting data is land surface temperature. Derivative analysis and 2D modeling carried out by forward modeling is one method that can strengthen the geothermal potential in the area. Based on the Land Surface Temperature map, the temperature around the geothermal prospect area is 22 – 25 ^{0}C. The results of the derivative analysis show that the geothermal prospect of Mount Hamiding is controlled by two different faults, a fault due to the depression of the old Hamiding caldera and a local fault under the surface of Mount Dukono, which is confirmed as a reverse fault. While the 2D modeling identified the geothermal reservoir layer, which is estimated to have a density of 1.59 gr/cc and consists of a mixture of tuff and minor lava, where the contents of this reservoir are water dominant due to the relatively low-density value with a depth of -411 – (-1280) m, above the reservoir layer it is suspected that the tuff and clay insert layer has a density of 2.56 gr/cc with a depth of 310 – (-1280) m, and the covering layer which is presumed to be a clay cap layer has a density of 1.39 gr/cc with a depth of 870 – (-620).

Keywords: Derivative Analysis; forward modelling; LST; gravity method; Geothermal

1. Introduction

Indonesia's dependence on fossil energy to meet domestic energy needs is still high. Fossil energy contributes 94.3% of the total national energy demand of 1,357 million BOE (barrel oil equivalent), while the remaining 5.7% is met from new and renewable energy. Dependence on fossil energy needs to end by utilizing alternative energy potentials that exist throughout Indonesia, such as hydropower, wind, geothermal, and biomass. The potential for alternative energy that is very promising to be utilized is geothermal because Indonesia has the largest reserves in the world, namely 40% [1].

A geothermal system is usually associated with volcanic systems formed along island arcs due to plate movement on the earth's surface that causes volcanoes to occur [2-4]. The main requirements for the formation of a geothermal (hydrothermal) system are a large heat source (heat source), a reservoir for accumulating heat, and a cap rock for accumulating heat. A productive geothermal reservoir must have high porosity and permeability, large enough size, high temperature, and sufficient fluid content. Cover rock that is impermeable or has low permeability covering the reservoir is needed to prevent the escape of hot fluid accumulation in the reservoir [5].

Supriatna (1980) states that stratigraphically, the oldest rock unit exposed in the West – North Halmahera area is the Weda Formation consisting of sandstone, claystone, siltstone, marl, limestone, and conglomerate. While the area of the Hamiding volcanic complex (G. Hamiding and G. Kao) may be related to heat sources that control the emergence of fumarole manifestations and surface alteration, rock units from the Togawa Formation (Qpt) may have potential as reservoir rocks in this area. The reservoir rocks are generally dominated by pyroclastic tuff and minor lava. The presence of warm springs in the Mamuya area can also indirectly indicate that Mount Mamuya also has the potential as a heat source, while Mount Dukono considering its status as an active volcano, almost certainly also has the potential as another heat source in this region [6].

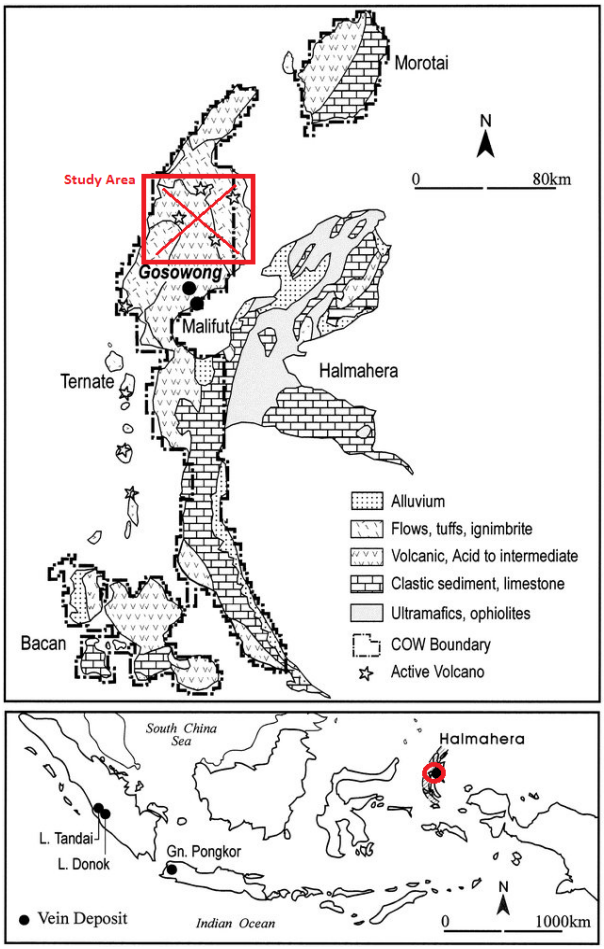

Figure. 1 Region Geology of Hamiding Mount. [4-5]

Newton's law expresses the force of gravitation; the force between two particles of masses m_1 and m_2 is directly proportional to the product of the masse and inversely proportional to the square of the distance between the centers of masses [7].

$$F = \gamma \left(\frac{m_1 m_2}{r^2}\right) r_1 \qquad (1)$$

The gravity method is processed to produce a Complete Bouguer Anomaly (CBA) value. The gravitational anomaly data obtained from the satellite is gravity anomaly data that has been corrected to free air correction, so the only correction needed is free air correction,

terrain correction, and Bouguer correction aimed at reducing rock mass in the earth's crust that lies between the plane of the spheroid and the measurement point [8].

Free air correction is a correction made because of the influence of altitude on the earth's gravitational field [9]. For FAC itself, it is obtained from 0.3085h, which is then combined with the previous correction so that the equation becomes:

$$FAA\ (R+h) = g_{obs} - g(R) + 0.3085h \quad (2)$$

With Free Air Anomaly, gobs are the observed gravitational acceleration, h indicates the corrected altitude, and g(R) is the latitude corrected gravitational acceleration value [10].

Bouguer correction is used to reduce the value of gravity due to the presence of rock mass between the measurement points at the height of h meters to MSL (Mean Sea Level) so that the measured value of gravity is greater than the value of gravity that should be on the equipotential surface [11].

$$BC = 0.000419\Delta h\rho \quad (3)$$

BC is the Bouguer correction (mGal), h is the difference between the height of the measurement point and the datum (m), and is the density (kg/m^3).

Terrain Correction is caused by the influence of material around the measurement point that contributes to the measurement results, so topographic correction must be carried out first if the measurement field has an irregular topography, such as a series of mountains or hills. The effect of gravity on a sector can be calculated by the following formula [12]:

$$TC = G\ \rho\ \theta\ [(r_2 - r_1) + \sqrt{r_1^2 + z^2}\sqrt{r_2^2 + z^2}\ ] \quad (4)$$

TC is Terrain Correction (mGal), G is universal constant, = Density of rock mass (kg/m^3), the angle formed by compartment (degrees), r radius of the inner circle (m), r radius of outer circle (m), z = Height of hill / depth of valley (m).

First Horizontal Derivative (FHD) has another name Horizontal Gradient. The horizontal gradient of the gravitational anomaly caused by a body tends to show the edges of the body (Zaenudin et al, 2013). So the horizontal gradient method can be used to determine the location of the horizontal density contrast contact boundary from gravity data (Cordell, 1979 in Zaenudin et al, 2013). To calculate the FHD value can be done with the equation [13]:

$$FHD = \frac{g_{(i+1)} - g_{(i)}}{\Delta x} \quad (5)$$

where g is anomaly value (mgal), x is the difference between the distance on the path (m), FHD is First Horizontal Derivative.

Second Vertical Derivative (SVD) can be used to assist the interpretation of the type of structure on the Bouguer anomaly data caused by the presence of a descending or rising fault structure. SVD acts as a high pass filter, so it can describe residual anomalies associated with shallow structures that can be used to identify the type of descending fault or ascending fault. [14] Theoretically, this method is derived from the Laplace equation so that the determination of the SVD value can be used by the second derivative with the equation:

$$SVD = \frac{g_{(i+1)} - 2g_{(i)} + g_{(i+1)}}{\Delta x^2} \quad (6)$$

Land surface temperature mapping is carried out to determine the spatial distribution area that affects the increase in ground surface temperature. Objects that have a low emissivity, low heat capacity, and high thermal conductivity will experience an increase in surface temperature, while on the contrary, will experience a decrease in surface temperature [15]. To obtain the Land surface temperature, the corrected emissivity Ts is calculated as follows:

$$Ts = \frac{BT}{\{1+[(\frac{\lambda BT}{\rho})\ln\lambda]\}} \quad (7)$$

Where Ts is the Land surface temperature in Celsius, BT on the BT sensor (°C), is the emitted emission wavelength (where the peak and average response of the wave boundary (λ = 10,895 (Markham & Barker, 1985) will be

used)), is the emissivity based on calculations by Weng et al. (2004) [16].

2. Experiments Procedure

This research was conducted in the area of Mount Hamiding, located in North Halmahera Regency, North Maluku Province, with an area of about 1818 km^2. Where this area includes the geothermal working area of Mount Hamiding, which is adjacent to Mount Dukono and Mount Mamuya, the stages of data processing can be seen in Figure 2.

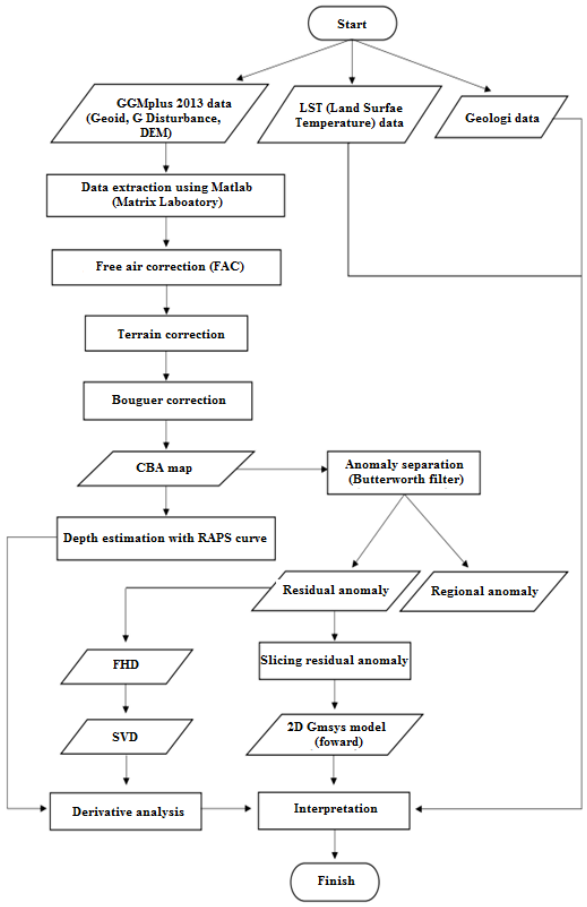

Figure. 2 Research Flowchartin this study

3. Result and Discussion

After the data has been corrected for free air, Bouguer correction, and field correction, the results obtained are Complete Bouguer Anomaly (CBA) which represents the distribution of gravity anomalies and the contrast of rock density in the study area, namely Mount Hamiding and its surroundings due to differences in density below the surface (Figure. 3).

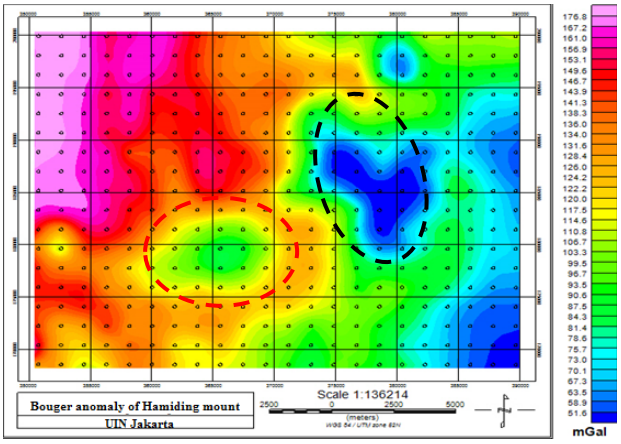

Figure 3. Complete Bouguer Anomaly (CBA) maps

It can be seen on the CBA map that the value of the gravity anomaly in the study area ranges from 51.6 – 176.8 mGal, where the low anomaly value (dark blue – light blue) ranges from 51.6 – 75.7 mGal, the medium anomaly value (dark green-yellow) ranges from 81.4 – 114.6 mGal and high anomaly values (orange – purple) ranged from 117.5 – 176.8 mGal. From the distribution of anomalies seen on the CBA map, it is clear that there are two anomalies that are clearly very unique. It can be seen that the medium anomaly surrounded by high anomalies is the old Hamiding caldera or caldera collapse, which controls the geothermal structure in the Hamiding Mountain area and its surroundings (red circle). . It is also seen that the low anomaly on the CBA map ranging from 51.6 – 75.7 mGal can be indicated as alteration rock around Mount Dukono.

If an overlay is done on the regional geological map and the CBA map (Figure 4), the area that has geothermal prospects can be divided into two areas; first, the area in the southwest is the Old Hamiding Caldera which has a Togawa Formation lithology (Qpt) which includes sandstone, tuff, conglomerate with andesite and basalt components. Then the second area in the northeast is the rock alteration area of Mount Dukono, which has a Holocene volcanic rock lithology (Qhva) which includes lava rock and andesite breccia.

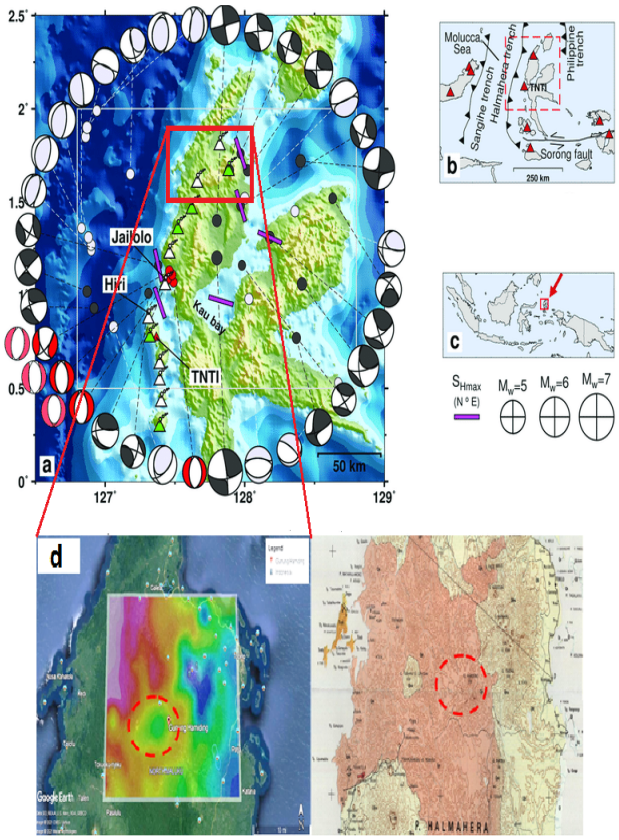

Figure 4. Map of Halmahera, tectonics, and strain/stress field [17]. **(a)** Map of the northern part of Halmahera island with topography and bathymetry from GEBCO_2014 grid version 20150318, www.gebco.net. Colored circles are the epicenters of the FMs reported in the GCMT catalog, selected within the region indicated by the light gray box and with <50 km hypocentral depth. Volcanoes are indicated with volcano symbols: green-colored symbols indicate Holocene eruptions, while white-colored symbols indicate unknown Holocene eruptions (Global Volcanism Program). The red triangle shows the TNTI seismic station. **(b)** A larger map indicates the main regional tectonic structures of the Molucca Sea and Halmahera region. Red triangles are the seismic stations of the Indonesian (IA) and GEOFON (GE) networks used in this study. The red box indicates the area plotted in (a). **(c)** Map of Indonesia highlighting the Halmahera region plotted in (a). **(d)** Interpretation of Bouger anomaly in the study area

The Land Surface Temperature map shows that the Mount Hamiding area and its surroundings have a surface temperature of around 22-25 ^{0}C where this surface temperature is still said to be quite ideal for geothermal locations (Figure 5).

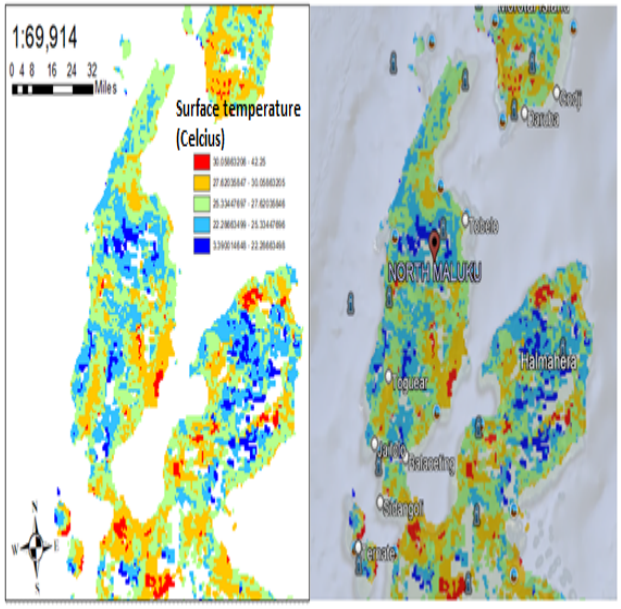

Figure 5. (a) Peta *Land Surface Temperature* (LST), and (b) *Overlay Map* LST and *Google Earth*

On the topographic map, it can be seen that the height of Mount Hamiding and its surroundings (Figure 6). On the topographic map, it can be seen that the height of the study area varies with a value of around -21.6 – 870 masl. The topographic map has one function to validate whether the Complete Bouguer Anomaly value is correct or not. In this study, the Complete Bouguer Anomaly value is valid because in the formulation of the gravity value, the height value is inversely proportional to the gravity acceleration value, the higher the surface, the smaller the gravity anomaly value [17-18].

The estimated depth obtained from the research data is approximately 3 km from the measurement point (Figure 7). In Figure 7, the depth is obtained from the analysis of the RAPS curve (Radially Average Power Spectrum) where it can be seen that the RAPS curve is decaying in shape where there are 2 zones, namely the regional zone where this zone is located in the part that has a steep slope gradient and the rest is the residual zone, in this case the

depth that is The depth of the regional zone used is 3 km from the measurement point

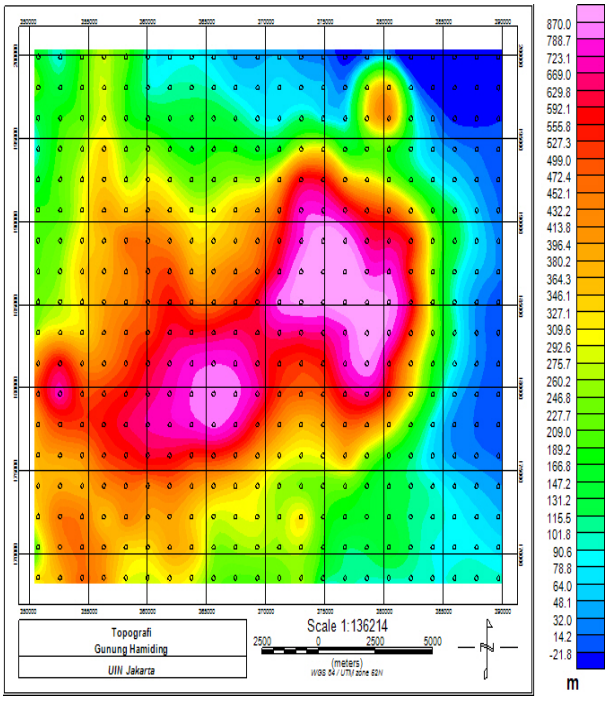

Figure 6. Topography Map

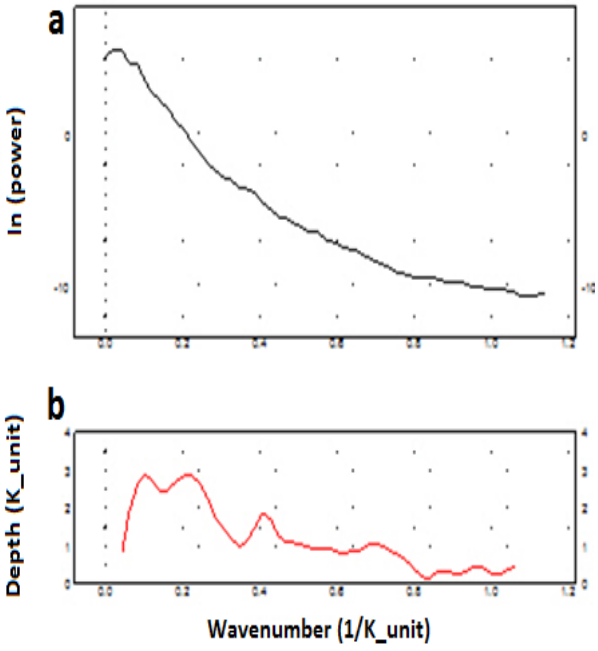

Figure 7. (a) Radially aveaged power spectrum. **(b)** Curve of Depth Estimate

After separating the anomalies using the Butterworth filter, residual anomalies (shallow anomalies) and regional anomalies (deep anomalies) will be generated (Figure 8).

It can be seen on the residual anomaly map (Figure 8.a), the heterogeneity of the distribution of the gravity anomaly on the surface is very visible because this anomaly is shallow caused by rocks or layers near the surface. Residual anomaly values in the study area ranged from -29.2 – 20.1 mGal, where low anomaly values ranging from -29.2 – (-8.1) mGal were the research targets marked in blue because the Hamiding geothermal system is a water-dominated system, where water has a low density value. There are two areas on the residual anomaly map, the first in the southwest direction shows that the geothermal system is controlled by the old Hamiding caldera or the caldera depression that forms a circle on Mount Hamiding (red circle) which causes fractures in the subsurface which become the transportation route in and out the fluid level and the second in the northeast direction is a low anomaly (black circle) which is estimated to be a weak zone or rock alteration zone under Mount Dukono. On the regional anomaly map (Figure 8.b) it can be seen that the distribution of the gravitational anomaly has very little heterogeneity on the surface because this anomaly is deep caused by rocks or layers deep in the earth's surface [20], Regional anomaly values in the study area ranged from 64 – 172.4 mGal.

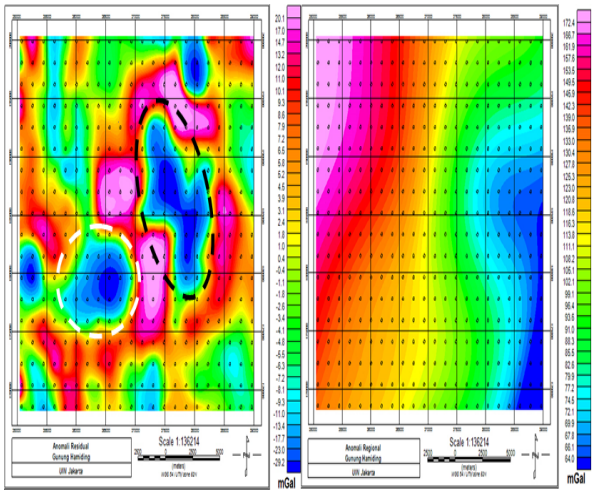

(a) (b)

Figure 8. (a) Residual Anomaly (b) Regional Anomaly

4. Analysis of Validation and Types of Fault

This analysis was carried out using the graphical correlation method between the First Horizontal Derivative (FHD) and Second Vertical Derivative (SVD) (Figure 10), FHD was performed to determine the boundary of the geological structure that caused the anomaly and SVD was performed to elicit shallow effects from regional influences or to determine type of fault in the study area.

In Figure 9 it is clear that the depression of the old Hamiding caldera and local faults around Mount Dukono on the FHD map are marked with high anomalies while on the SVD map it can be seen that the depression of the old Hamiding caldera and local faults around Mount Dukono are characterized by low anomalies, it can be concluded that the presence of the old Hamiding caldera depression and local faults around Mount Dukono can be well confirmed on FHD and SVD maps.

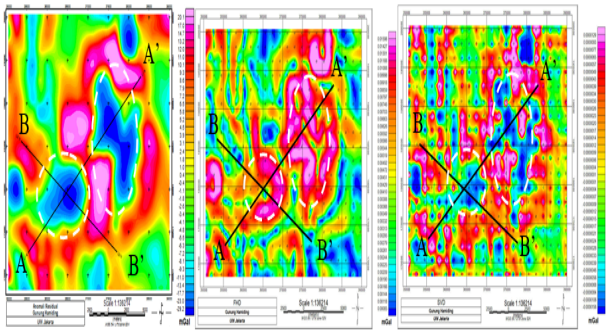

(a) (b) (c)

Figure 9. Fault Indication Area**:** (a) Anomaly of Residual (b) SVD (c) FHD

From the results of the correlation between the FHD and SVD graphs (Figure 10), it can be seen that there are five faults on line A – A' and three faults on line B – B'. According to fault analysis on line A – A', the first fault (P_1) is located at UTM coordinates (357494.9, 174222.2) with normal fault characteristics because the SVD max value > SVD min value where the min SVD value is -0.12 and the max SVD value is 0.37. The second fault (P_2) is at UTM coordinates (358941.4, 175293.4) with an increasing fault characteristic because the SVD min value > SVD max value where the min SVD value is -1.45 and the max SVD value is -0.03. The third fault (P_3) is at the coordinates of UTM (368303.6, 182226.8) with an increasing fault characteristic because the SVD min value > SVD max value where the min SVD value is -0.51 and the max SVD value is 0.33. From the results of these three faults, it is suspected that they are the result of depression of the Old Hamiding Caldera. The fourth fault (P_4) is at the UTM coordinates (370513.6, 183863.4) with an increasing fault characteristic because the min SVD value > SVD max value where the min SVD value is -0.89 and the max SVD value is 0.33. The fifth fault (P_5) is at the coordinates of UTM (377063.1, 188713.8) with an increasing fault characteristic because the min SVD value > SVD max value where the min SVD value is -0.87 and the max SVD value is 0.25. These two faults are thought to be local faults around Mount Dukono.

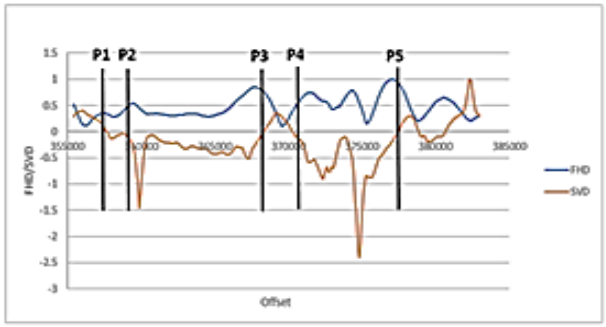

(a)

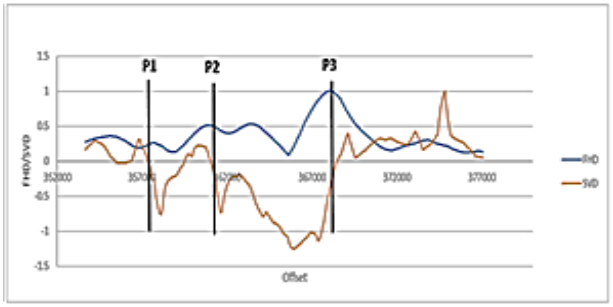

(b)

Figure 10. Graph Correlation Analysis of FHD vs SVD**: (a)** Slicing A – A' **(b)** Slicing B – B'

According to fault analysis on line B – B', the first fault (P_1) is at UTM coordinates (357515.6 , 183494.6) with increasing fault characteristics because the SVD min value > SVD max value where the min SVD value is -0.76 and the max SVD value is 0.28. The second fault (P_2)

is at UTM coordinates (361285.2 , 181425.7) with an increasing fault characteristic because the min SVD value > SVD max value where the min SVD value is -0.73 and the max SVD value is 0.22. The third fault (P_3) is at the UTM coordinates (368298.3, 177576.5) with an increasing fault characteristic because the SVD min value > SVD max value where the min SVD value is -1.14 and the max SVD value is 0.35. These three faults are thought to be the result of depression of the old Hamiding caldera.

This 2D modeling was carried out in two slicing on the residual anomaly map aimed at validating the results of 2D modeling, the first slicing is trending from southwest to northeast (A – A') (SW - NE) and the second slicing is trending northwest to southeast (B – B') (NW – SE), the slice selection is based on a low anomaly target or what is indicated is a reservoir layer that is dominated by liquid fluid where the liquid fluid has a low density (Figure 11).

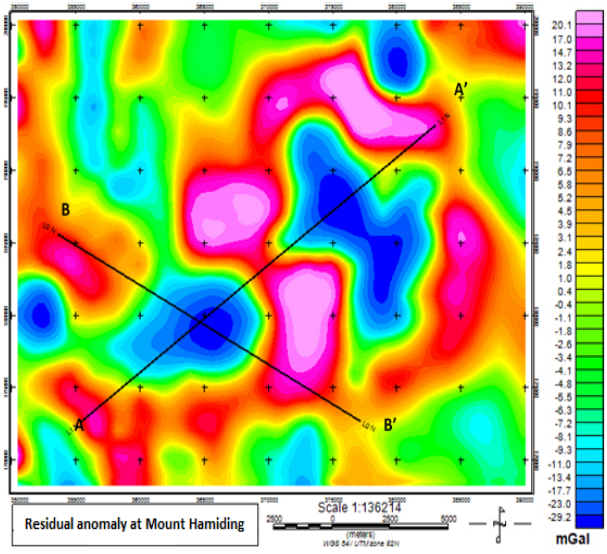

Figure 11. Slicing on Residual Anomaly Maps

The first slicing model is from Southwest to Northeast (A - A') (SW - NE) (Figure 12) where the slicing passes through two geothermal system objects, namely Mount Hamiding and Mount Dukono , it can be seen in the 2D modeling that there are 3 constituent layers hot system, namely clay cap with a density of 1.38 gr/cc with a depth of 870 – (-620) m as a covering layer, tuff and clay inserts with a density of 2.56 gr/cc with a depth of 320 – (-1280) m, tuff and minor lava with a density 1.59 gr/cc with a depth of – 620 – (-1280) m as reservoir layer. It can be seen that the upflow zone is located on Mount Hamidiing and can be seen the fault structure caused by the depression of the old Hamidiing caldera and local faults around Mount Dukono which control the geothermal system.

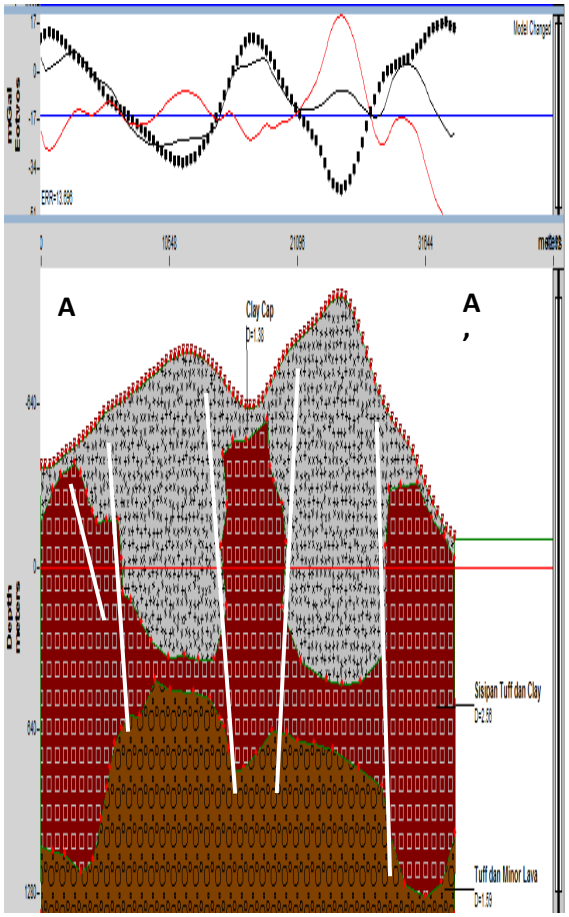

Figure 12. Northwest to Southeast 2D Modeling

The second slicing model is northwest to southeast (B – B') (NW - SE) (Figure 13) where the slicing is through the old Hamiding caldera or the Mount Hamiding caldera depression which controls the geothermal system, it can be seen in the 2D modeling that there are 3 constituent layers hot system, namely clay cap with a density of 1.38 gr/cc with a depth of 788.7 – (-306) m as a covering layer, tuff inserts and clay with a density of 2.56 gr/cc with a depth of 310 – (-1222) m , tuff and minor lava with a

density of 1.59 gr/cc with a depth of – -411 – (-1222) m as reservoir layer. It can be seen that the upflow zone is located on Mount Hamiding and it can be seen that the fault structure caused by the depression of the old Hamiding caldera can be seen.

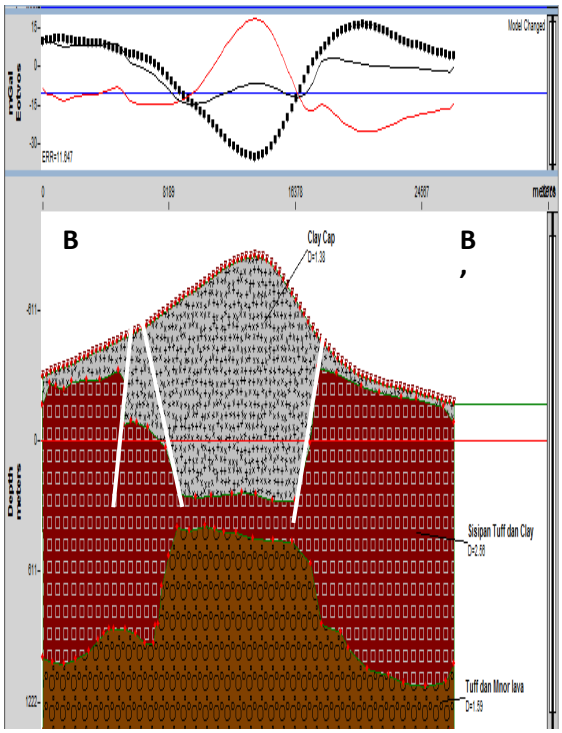

Figure 13. Northwest to Southeast 2D Modeling

5. Conclusion

Based on the results of research conducted with gravity in the area of Mount Hamiding, it can be concluded that: the residual anomaly target value in the study area ranges from -29.2 – 20.1 mGal, where the low anomaly value ranges from -29.2 – (-8.1) mGal to the research target because the Hamiding geothermal system is a water domination system, where water has a low-density value. The geothermal prospect of Mount Hamiding is controlled by the old Hamiding caldera in the form of a caldera depression which causes a local fault with an ascending fault type and other local faults around Mount Dukono with an ascending fault type, where the temperature around the geothermal prospect area is 22 – 25 C according to the ESG map.

In 2D forward modeling where the geothermal reservoir layer is estimated to have a density of 1.59 gr/cc which consists of a mixture of tuff and minor lava where the contents of this reservoir are water dominant due to the relatively low density value with a depth of -411 – (-1280) m, above the reservoir layer, it is suspected that there is an insertion layer of tuff and clay which has a density of 2.56 gr/cc with a depth of 310 – (-1280) m and a covering layer which is assumed to be a clay layer which has a density of 1.39 gr/cc with a depth of 870 – (-620) m.

Acknowledgment

The author gratefully ancknowledge the use of service and facilities at Universitas Islam Negeri Syarif Hidayatullah Jakarta, PT. Minelog Service Indonesia, and Kwansei Gakuin University.

References

[1] Regina, dkk. 2017. *"Panas Bumi Sebagai Harta Karun Untuk Menuju Ketahanan Energi".* Jurnal Ketahanan Nasional, Vol.23, No.2, Hal 217-237.

[2] Dian dan Rustadi. 2019. *"Interpretasi Sistem Panas Bumi Suwawa Berdasarkan Data Gaya Berat".* Jurnal Geofisika Eksplorasi, Vol. 5, No. 2, Hal. 44-54.

[3] Y. Daud et al., "Resistivity characterization of the Arjuno-Welirang volcanic geothermal system (Indonesia) through 3-D Magnetotelluric inverse modeling," Journal of Asian Earth Sciences, vol. 174, pp. 352–363, May 2019, doi: 10.1016/j.jseaes.2019.01.033.

[4] M. Alonso et al., "Thermal energy and diffuse 4He and 3He degassing released in volcanic-geothermal systems," Renewable Energy, vol. 182, pp. 17–31, Jan. 2022, doi: 10.1016/j.renene.2021.10.016.

[5] Kasbani. *"Tipe Sistem Panas Bumi Di Indonesia Dan Estimasi Potensi Energinya".* Kelompok Program Penelian Panas Bumi, PMG –Badan Geologi.

[6] Direktorat Jenderal EBTKE. 2017. *Potensi Panas Bumi Indonesia Jilid 1*. Jakarta: Direktorat KESDM.

[7] Carlile J. C., Davey G. R., Kadir I., Langmead R. P., Rafferty W. J. 1998. "*Discovery and exploration of the Gosowong epithermal golddeposit, Halmahera, Indonesia*", Journal of Geochemical Exploration. vol. 60, No 3, pp. 207 – 227, doi: 10.1016/S0375-6742(97)00048-4

[8] Telford, Geldert, Sheriff. 1990. "*Apllied Geophysics Second Edition"*. Cambride University Press : New York.

[9] D. Kucharski et al., "Full attitude state reconstruction of tumbling space debris TOPEX/Poseidon via light-curve inversion with Quanta Photogrammetry," Acta Astronautica, vol. 187, pp. 115–122, Oct. 2021, doi: 10.1016/j.actaastro.2021.06.032.

[10] P. Kunnummal and S. P. Anand, "Qualitative appraisal of high resolution satellite derived free air gravity anomalies over the Maldive Ridge and adjoining ocean basins, western Indian Ocean," Journal of Asian Earth Sciences, vol. 169, pp. 199–209, Jan. 2019, doi: 10.1016/j.jseaes.2018.08.008.

[11] H. Ryka and R. S. Afifah. 2019. "*Pemodelan Geologi Bawah Permukaan Bantar Karet, Jawa Barat Menggunakan Metode*," vol. 3, no. 2, pp. 59–65, 2019, doi: 10.20956/geocelebes.v3i2.6689.

[12] Aji D. M. 2019. *"Analisa Matematis pada Koreksi Bouguer dan Koreksi Medan Data Gravitasi Satelit Topex dalam Penentuan Kondisi Geologi Studi Kasus Sesar Palu Koro, Sulawesi Tengah".* Jurnal Geosaintek, Vol. 5, No. 3, pp. 91-100.

[13] Yulistina, S. 2017. *"Studi Identifikasi Struktur Geologi Bawah Permukaan Untuk Mengetahui Sistem Sesar Berdasarkan Analisis First Horizontal Derivative (Fhd), Second Vertical Derivative (Svd), Dan 2,5d Forward Modeling Di Daerah Manokwari Papua Barat".* Universitas Lampung.

[14] Yasrifa, dkk. 2019. *"Pendugaan Patahan Daerah "Y" berdasarkan Anomali Gayaberat dengan Analisis Derivative".* Jurnal Geofisika Eksplorasi, Vol. 5, No. 1, Hal, 75-88.

[15] Triani T., Umam R., Sismanto S. 2021. "*3D Modeling of Subsurface Lawanopo Fault In Southeast Sulawesi, Indonesia Using Grablox and its Consequence to Geohazard*". The Indonesian journal of geography. Vol. 53. No. 1. pp. 67-77. doi: 10.22146/ijg.50878

[16] Brandon, dkk. 2021. *"Pengolahan Data Landsat Dan Gravitasi Sebagai Indikasi Panasbumi Daerah Rana Kulan, Ntt"*. JGE (Jurnal Geofisika Eksplorasi), Vol. 07 No. 1, Hal. 41-51.

[17] Passarelli L, Heryandoko N, Cesca S,Rivalta E, Rasmid, Rohadi S, Dahm Tand Milkereit C. 2018. "*Magmatic or Not Magmatic? The 2015–2016 Seismic Swarm at the Long-Dormant Jailolo Volcano, West Halmahera,Indonesia*". Front. Earth Sci. Vol 6, No. 79. pp 1-17. doi: 10.3389/feart.2018.00079

[18] Prastowo R., Helmi H., Trianda O., Umam R. 2021. *"Identification of Slip Surfaces Using the Geoelectric Imaging Method in the Kalirejo Area, Kokap District, Yogyakarta, Indonesia"*. JIPF (Jurnal Ilmu Pendidikan Fisika). Vol. 6. No. 3. pp. 2477-8451. doi: 10.26737/jipf.v6i3.2072

[19] Prastowo R., Helmi H., Trianda O., Umam R. 2021. *"Identification of Andesite Resource Potential In Kalirejo Area, Kokap Sub-District, Kulon Progo Using Resistivity Method"*. Forum Geografi Vol. 35. No. 1. pp: 74-84. doi: 10.23917/forgeo.v35i1.13507

[20] Anwar H., Ipmawan V. L., Sriyakul T. 2022. *"Geophysical Analysis Using Proton Precession Magnetometer GSM-19T as Information on Fault Presence in Medana, North Lombok, Indonesia"*. International Journal of Hydrological and Environmental for Sustainability (IJHES). Vol. 1. No. 1. pp. 8-23.